

# Parafermions in a multi-legged geometry: Towards a scalable parafermionic network

Udit Khanna,<sup>1,2,3</sup> Moshe Goldstein,<sup>1</sup> and Yuval Gefen<sup>2</sup>

<sup>1</sup>Raymond and Beverly Sackler School of Physics and Astronomy, Tel Aviv University, Tel Aviv 6997801, Israel

<sup>2</sup>Department of Condensed Matter Physics, Weizmann Institute of Science, Rehovot 76100, Israel

<sup>3</sup>Present Affiliation: Department of Physics, Bar-Ilan University, Ramat Gan 52900, Israel

Parafermionic zero modes are non-Abelian excitations which have been predicted to emerge at the boundary of topological phases of matter. Contrary to earlier proposals, here we show that such zero modes may also exist in multi-legged star junctions of quantum Hall states. We demonstrate that the quantum states spanning the degenerate parafermionic Hilbert space may be detected and manipulated through protocols employing quantum anti-dots and fractional edge modes. Such star shaped setups may be the building blocks of two-dimensional parafermionic networks.

**Introduction.** Parafermion (PF) zero modes are fractionalized excitations with non-Abelian statistics, which may exist at the boundary of certain topological phases of matter [1]. PF zero modes are expected to show a number of interesting phenomena [2–21] such as the fractional Josephson effect, zero-bias anomaly, and topological Kondo effect, and may be potentially useful in quantum information applications [5, 22–30]. General classifications of truly one-dimensional (1D) bosonic and fermionic systems rule out the existence of PFs beyond Majorana zero modes [31–34]. However, PF zero modes may be supported at suitably designed line junctions at the boundary of fractional quantum Hall (QH) states [2–4]. In particular, two counter-propagating chiral edge modes with opposite spins, at the interface of FQH puddles in the  $\nu = 1/m$  state, may be gapped by proximity to a bulk superconductor or a ferromagnet. The domain walls between superconducting and ferromagnetic segments are expected to host  $\mathbb{Z}_{2m}$  PF zero modes on the boundary [2, 3]. Similar setups have been proposed for the  $\nu = 2/3$  state [5], in hierarchical [35] and bilayer [36–38] fractional QH phases, in proximitized and fractional topological insulators [11, 20, 39–44], as well as in systems of coupled 1D wires [45–52]. Such PF modes can be detected through their transport signatures in appropriately designed setups [7, 21, 38, 53, 54]. 2D parafermionic networks are predicted to host even more exotic Fibonacci anyons, which may eventually allow fault-tolerant universal quantum computation [5, 6, 55, 56].

Here we propose a setup hosting PF zero modes, based on multi-legged star junctions of FQH states. Figure 1 shows the simplest such geometry supporting a parafermionic zero mode localized at the center of the star junction. Such a geometry may be based on single layer FQH states [2, 3] employing superconducting regions [Fig. 1(a)] or double layer states [36, 37] employing interlayer electron tunneling at the interfaces [Fig. 1(b)]. Similar setups have been studied previously in the context of Majorana zero modes (which are  $\mathbb{Z}_2$  PFs) localized at the boundaries of 1D nanowires [57–65]. These studies found that a single zero energy Majorana mode is supported at the center of odd-legged star junctions, but not in the case of even number of legs. The present

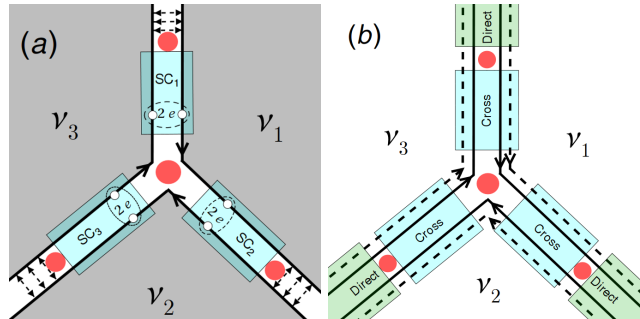


FIG. 1. Trijunctions hosting parafermionic zero modes (represented by red circles) may be constructed in (a) single-layer or (b) double-layer setups. The black lines represent the chiral edge modes of the three quantum Hall puddles. In (b), the solid (dashed) lines represent the edge modes of the top (bottom) layer. Counter-propagating pairs of edge modes may be gapped out by introducing superconducting or electron-tunneling segments in the single-layer setup [Panel (a)]. In the bilayer setup [Panel (b)], edge modes may be gapped out by introducing segments with direct (intra-layer) or crossed (inter-layer) electron-tunneling.

work is a concrete extension of the previous studies to the case of  $m > 1$  PF modes, which requires one to consider interacting systems. Here, one might naively expect a modulo  $2m$  dependence on the number of wires. In contrast, we interestingly find the modulo 2 behavior to persist, namely that parafermionic junctions with an odd (even) number of legs would (would not) host a single parafermion at the center of the star which cannot (can) be gapped out. Below we analyse the low energy dynamics of a trijunction geometry, demonstrating the existence of parafermionic zero mode and the degeneracy of the zero energy Hilbert space. Furthermore, we propose specific setups employing quantum anti-dots (QADs) and fractional edge modes, which may be used to measure the degeneracy of the parafermionic Hilbert space and facilitate manipulation of such states.

**Trijunction Model.** We consider a single trijunction setup [Fig. 1(a)] comprising the boundary of three  $\nu_j = \nu = \frac{1}{m}$  ( $j = 1, 2, 3$ ) QH puddles with same spin polarization. The low-energy dynamics of each puddle is governed by a chiral edge mode, described by a bosonic

field  $\phi_j(x, t)$  [66]. These bosonic fields are described by the Hamiltonian

$$H_{\text{edge}} = \frac{mv}{4\pi} \sum_{j=1}^3 \int dx [\partial_x \phi_j(x)]^2, \quad (1)$$

where  $v$  is the edge mode velocity (assumed to be identical, for all puddles, for simplicity) and satisfy

$$[\phi_j(x), \phi_j(y)] = \frac{i\pi}{m} \text{sgn}(x - y), \quad (2)$$

$$[\phi_j(x), \phi_k(y)] = i \frac{\pi}{m} \text{ for all } j > k. \quad (3)$$

Here the coordinate  $x$  increases along the direction of propagation for each edge mode. The second commutator above relies on the assumption that the edge modes are segments of a single boundary. At the center of the trijunction, each pair of counter-propagating edge modes is gapped out through proximity coupling to a  $p$ -wave superconductor [67]. The superconducting regions are described by,

$$H_s = \Delta \sum_j \int dx \cos [m(\phi_j + \phi_{j-1}) + \hat{\varphi}], \quad (4)$$

where  $\phi_0$  has been identified with  $\phi_3$ , and we assume the amplitude ( $\Delta$ ) and phase ( $\varphi$ ) of all superconducting segments to be identical. This is possible if all three segments are generated by proximity to the same bulk superconductor. In order to fix the boundary conditions and the total charge hosted by the setup, we also assume that (away from the junction) each pair of counter-propagating modes is gapped out through strong interedge electron tunneling [denoted as black dashed double-headed arrows in Fig. 1(a)]. The tunneling regions are described by

$$H_t = g \sum_j \int dx \cos [m(\phi_j - \phi_{j-1})]. \quad (5)$$

Finally, we assume that the superconducting segments (implicitly assumed to be part of the same bulk superconductor) are floating. Their total charge ( $Q_T$ ) appears in the Hamiltonian as a charging term,  $(\hat{Q} - Q_T)^2/2C$ , where  $\hat{Q} = \sum_j \hat{Q}_j$  is the total charge and  $\hat{Q}_j$  is the charge hosted in the  $j^{\text{th}}$  superconducting segment, and is given by

$$\hat{Q}_j = \frac{1}{2\pi} \int_{\text{SC}_j} dx (\partial_x \phi_j - \partial_x \phi_{j-1}). \quad (6)$$

Since the (total) charge and phase of the superconductor are conjugate variables, they satisfy  $[\hat{\varphi}, \hat{Q}] = 2i$ .

We restrict our analysis to energies below  $\sqrt{4\pi mv\Delta}$  and  $\sqrt{4\pi mv g}$ . In this limit, the fractional chirals may be assumed to be completely pinned inside the superconducting and tunneling segments [3]. It follows that the

superconducting and tunneling regions are described by integer-valued operators  $\hat{N}_j$  and  $\hat{M}_j$  respectively. Therefore at each boundary of the trijunction, we must have

$$\phi_j + \phi_{j-1} = \frac{2\pi}{m} \hat{N}_j, \quad (7)$$

where  $\hat{N}_j \rightarrow \hat{N}_j + \hat{\varphi}/m$ . Similarly, at each boundary of the tunneling regions we have

$$\phi_j - \phi_{j-1} = \frac{2\pi}{m} \hat{M}_j. \quad (8)$$

Our next task is to analyze the low lying dynamics of this trijunction block showing that it exhibits parafermionic physics. To this end, we perform a standard mode expansion of the chiral fields,

$$\phi_j(x, t) = \varphi_j + A_j p_{\varphi_j} (vt - x) + \sum_{n>0} \left[ B_{nj} a_{nj} e^{-iq_{nj}(vt-x)} + \text{h.c.} \right], \quad (9)$$

where  $A_j$  and  $B_{nj}$  are  $c$ -numbers and  $a_{nj}$  describe the bosonic excitations in the chiral modes. Imposing the boundary conditions [Eq. (7)] and commutation relation [Eq. (2)] inside the trijunction, we find

$$\phi_1(x, t) = \varphi_1 + \sqrt{\frac{2}{m}} \sum_{n>0} \left[ \frac{a_n}{\sqrt{2n-1}} e^{-iq_n(vt-x)} + \text{h.c.} \right], \quad (10)$$

$$\phi_2(x, t) = -\phi_1(x + L_1, t) + \varphi_1 + \varphi_2, \quad (11)$$

$$\phi_3(x, t) = -\phi_2(x + L_2, t) + \varphi_2 + \varphi_3, \quad (12)$$

where  $\varphi_j = \frac{\pi}{m} (\hat{N}_j + \hat{N}_{j+1} - \hat{N}_{j-1})$  (not to be confused with  $\hat{\varphi}$ ),  $q_n = (2n-1)\frac{\pi}{\ell}$ ,  $L_j$  is the length of the  $j^{\text{th}}$  chiral inside the trijunction, and  $\ell = \sum_j L_j$ . A similar expansion can be performed for the region between the superconductor and the tunneling segments [2].

Plugging the expansion found above into Eq. (3), we find that the only non-zero commutation relations are,

$$[\hat{N}_3, \hat{N}_2] = \frac{im}{\pi} \quad \text{and} \quad (13)$$

$$[\hat{N}_1, \hat{M}_1] = [\hat{N}_2, \hat{M}_1] = [\hat{N}_3, \hat{M}_1] = \frac{im}{\pi}. \quad (14)$$

Using (6), the charge on the superconducting segments (at low energies) is found to be

$$\hat{Q}_j = \frac{1}{m} (\hat{N}_{j+1} - \hat{N}_{j-1} - \hat{M}_j). \quad (15)$$

Note that the total charge  $\hat{Q} = -\sum_j \hat{M}_j$  depends only on the integers describing the electron-tunneling regions at the boundaries. Since the charge on each superconducting segment is defined module 2, the physical operators to consider are  $e^{i\pi\hat{Q}_j}$ . These satisfy

$$e^{i\pi\hat{Q}_j} e^{i\pi\hat{Q}} = e^{i\pi\hat{Q}} e^{i\pi\hat{Q}_j} \quad \text{and} \quad (16)$$

$$e^{i\pi\hat{Q}_{j-1}} e^{i\pi\hat{Q}_j} = e^{i\frac{\pi}{m}} e^{i\pi\hat{Q}_j} e^{i\pi\hat{Q}_{j-1}} \quad \text{for all } j. \quad (17)$$

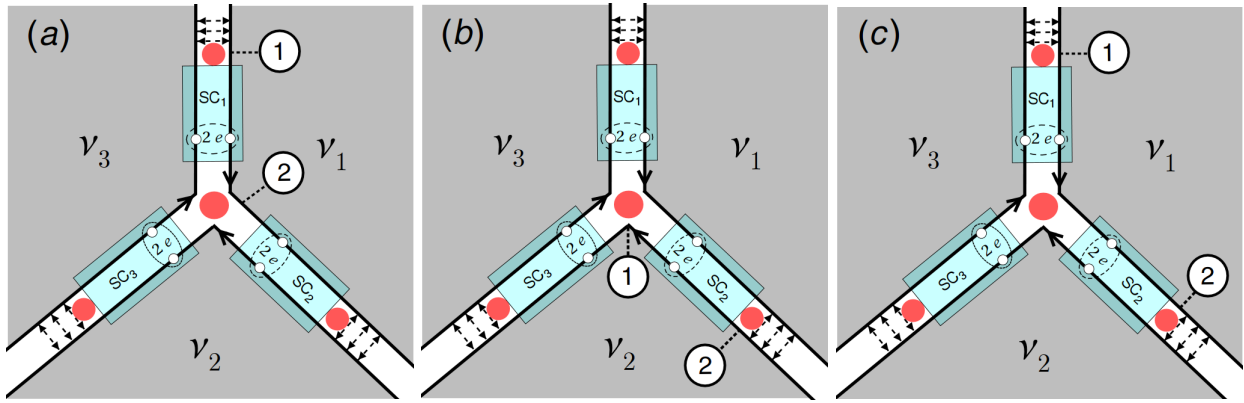


FIG. 2. Schemes for state manipulation in the trijunction (adopted from Ref. [53]). The white circles denote quantum anti-dots which may host a single Laughlin quasiparticle and are tunnel-coupled to one of the interfaces supporting a parafermionic mode. As described in the text, the state of the trijunction may be manipulated through the application of operators of the form  $e^{\pm i\pi\hat{Q}_j}$  ( $j = 1, 2, 3$ ). Varying the gate voltage on the anti-dots in an adiabatic fashion allows for the application of (a)  $e^{\pm i\pi\hat{Q}_1}$ , (b)  $e^{\pm i\pi\hat{Q}_2}$  and (c)  $e^{\pm i\pi(\hat{Q}_1 + \hat{Q}_2)} \sim e^{\pm i\pi(\hat{Q} - \hat{Q}_3)}$ . Moving the anti-dots to the opposite side of the same interface would modify the operator by an overall phase.

Finally, we may write the Hamiltonian of the trijunction (ignoring the charging term for now) as,

$$H = H_{\text{edge}} + H_s + H_t = \sum_{n>0} v q_n (a_n^\dagger a_n + \frac{1}{2}) \quad (18)$$

Note that  $H$  only depends on the bosonic excitations of the chiral fields and not on  $\hat{N}$ . This allows for the possibility that the Hamiltonian supports zero energy solutions. To this end, we construct operators which commute with the Hamiltonian and describe (local) superpositions of quasiholes and quasiparticles in the chiral edge modes. A quick calculation confirms that the operator  $\tilde{\Gamma}$  defined as,

$$\tilde{\Gamma}_0 = e^{i\varphi_1} \int dx \sum_{k=1}^3 [e^{-i\varphi_k} e^{i\phi_k(x)} + \text{h.c.}] \quad (19)$$

satisfies these requirements [68]. We may define  $\Gamma_0 = e^{i\varphi_1} = e^{i\frac{\pi}{m}(\hat{N}_1 + \hat{N}_2 - \hat{N}_3)}$  as the projection of  $\tilde{\Gamma}_0$  onto the ground state (in the absence of bosonic fluctuations). Similar expressions can be defined for the three zero modes ( $\Gamma_j$ ) localized at the domain wall between the ( $j^{\text{th}}$ ) superconducting segment and corresponding tunnel junction at the boundary of the trijunction. Therefore the low-energy physics of the trijunction is governed by the four localized zero energy modes which satisfy parafermionic commutation relations,  $\Gamma_\alpha \Gamma_\beta = e^{i\frac{\pi}{m}} \Gamma_\beta \Gamma_\alpha$  if  $\alpha$  appears to the left of  $\beta$  in the tuple  $(1, 0, 2, 3)$ . We note that there are multiple ways to represent the PF zero modes, which are localized at the different boundaries of the junction (for instance,  $\Gamma_0$  as defined above is localized at  $\phi_1$ ). Here we have used the convention that  $\Gamma_j$  ( $j = 1, 2, 3$ ) is localized at  $\phi_j$ .

The low-energy subspace of the trijunction is expected to be degenerate due to the PF commutation relations of

the zero modes. Since the operators  $e^{i\pi\hat{Q}_j}$  commute with  $H$ , the different states in the ground state sector may be labelled through their eigenvalues. The non-trivial commutations among these operators imply that the Hilbert space is spanned by states of the form  $|Q_T, Q_j\rangle$  (for a fixed  $j$ ). Since  $e^{i\pi\hat{Q}_j}$  can assume  $2m$  values, the total degeneracy of the ground state of the trijunction is  $(2m)^2$ , which is consistent with the presence of four  $\mathbb{Z}_{2m}$  PF modes. Note that the energy of states with different  $Q_T$  is set externally through the charging term in the Hamiltonian [which was ignored in eq. (18)]. Therefore the degeneracy of such states is lifted for finite charging energy. By contrast, the  $2m$  states with a given  $Q_T$  are degenerate up to exponentially small splittings (arising from the finite length of the superconductor) [69] which are neglected here.

Our analysis of the trijunction may be extended to star-shaped setups with a larger number of legs. The results are qualitatively unaltered for stars with an odd number of legs. On the other hand, for even-legged junctions, the low energy Hamiltonian of the junction [ $H$  in Eq. (18)] involves additional terms which explicitly depend on the integer-valued operators  $\hat{N}_j$ . Such terms rule out the possibility of a  $\mathbb{Z}_{2m}$  PF zero mode at the center of an even-legged junctions. Our results are also applicable to star-shaped junctions in bilayer setups. Specifically, a trijunction comprising the edge of QH bilayer [Fig. 1(b)] with  $\nu = 1/m$  per layer would host a  $\mathbb{Z}_m$  PF zero mode at its center.

*Ground state manipulation.* Here we discuss protocols (adopted from Ref. [53]) to induce transitions between the degenerate low-energy states of the trijunction. As described above, the total charge of the trijunction ( $Q_T$ ) is fixed externally through the charging energy. However, the degenerate states within a topological sector (labelled by  $Q_T$ ), may be manipulated through redistribu-

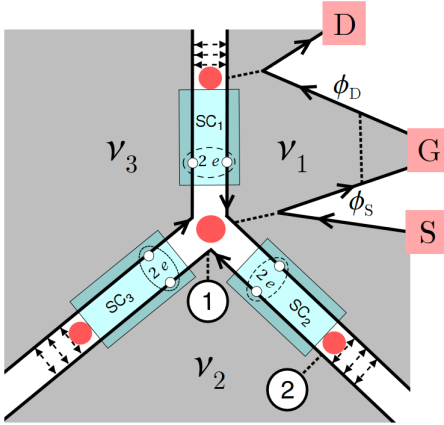


FIG. 3. Scheme for measuring the degeneracy of the trijunction (adopted from Ref. [53]). The white circles denote quantum anti-dots which facilitate the application of  $e^{\pm i\pi\hat{Q}_2}$  upon the trijunction state.  $\phi_{S/D}$  are additional fractional edge modes tunnel-coupled to the trijunction and to each other. Quasiparticles emanated from the source ( $S$ ) may end up at the drain ( $D$ ), by directly tunneling from  $\phi_S$  to  $\phi_D$ , or by tunneling across the trijunction. The interference between these two processes, and therefore the current ( $I_t$ ) from  $S$  to  $D$ , is sensitive to the state of the trijunction. Therefore repeatedly applying  $e^{i\pi\hat{Q}_2}$  through the anti-dots and monitoring  $I_t$ , allows one to measure the number of degenerate states in the parafermionic Hilbert space of the trijunction (for a fixed total charge).

tion of the charge among the superconducting segments. Suppose  $|\Psi\rangle$  is an eigenstate of  $e^{i\pi\hat{Q}_1}$  with eigenvalue  $e^{i\pi Q_1} = 1$ ; Eqs. (15-16) then imply that  $(e^{i\pi\hat{Q}_2})^k|\Psi\rangle$  is also an eigenstate of  $e^{i\pi\hat{Q}_1}$  with eigenvalue  $e^{i\frac{\pi k}{m}}$ . Therefore one may induce transitions between  $|Q_T, Q_1\rangle$  and  $|Q_T, Q_1 + \frac{1}{m}\rangle$  through the application of  $e^{i\pi\hat{Q}_2}$ . Similarly, application of  $e^{i\pi\hat{Q}_3}$  induces transitions from  $|Q_T, Q_1\rangle$  to  $|Q_T, Q_1 - \frac{1}{m}\rangle$ .

Figure 2 depicts several setups involving two QADs coupled to the trijunction, which may be used to apply the operators  $e^{i\pi\hat{Q}_j}$ . We assume that each QAD may be empty or host a single Laughlin quasiparticle depending on the voltage applied. Thus effectively each QAD can be modelled by a two-level system with the Hamiltonian,

$$H_{\text{QAD}} = V_Q \left( N_\psi - \frac{1}{2} \right), \quad (20)$$

where  $V_Q$  is proportional to the electrostatic potential on the QAD and  $N_\psi$  is the number of quasiparticles in the QAD. The tunnel-coupling of the QADs to the PF modes in the trijunction may be described by,

$$H_{\text{tun}} = \sum_{k=1,2} \tilde{J}_k \psi_k \Gamma_k^\dagger + \text{h.c.}, \quad (21)$$

where  $\psi_k$  is the quasiparticle operator for the  $k^{\text{th}}$  QAD satisfying  $[N_{\psi_k}, \psi_k] = -\psi_k$ , and  $\Gamma_k$  is the PF operator

coupled to the QAD. Since the PF modes have multiple representations (which are localized at different edges), here  $\Gamma_k$  is assumed to be localized at the boundary of the QH region in which the QAD is located. We assume that the tunneling amplitudes ( $\tilde{J}_k$ ) are much smaller than the charging energy of the trijunction ( $E_c$ ) so that  $H_{\text{tun}}$  leads to cotunneling of quasiparticles between the QADs, which may be described by,

$$H_{\text{co-tun}} = J \psi_1 \psi_2^\dagger \Gamma_1^\dagger \Gamma_2 + \text{h.c.} \quad (22)$$

Here  $J \sim \tilde{J}_1 \tilde{J}_2^*/E_c$  for  $E_c \gg \tilde{J}_{1,2}$ . Let us assume that the QADs were initially decoupled from the trijunction and prepared such that one QAD is occupied while the other is empty. Then by coupling them to the trijunction and slowly varying the voltage on the dots, we may induce the transition  $|\Psi\rangle \rightarrow \Gamma_1^\dagger \Gamma_2 |\Psi\rangle$ . Using equations (13-15), we find that the terms of the form  $\Gamma_0 \Gamma_j^\dagger$  are proportional to the operators  $e^{i\pi\hat{Q}_j}$ . We may facilitate the application of any operator ( $e^{i\pi\hat{Q}_j}$ ) through suitable placement of the two QADs. The setups shown in Fig. 2(a-c) may be used to realise  $e^{i\pi\hat{Q}_1}$ ,  $e^{i\pi\hat{Q}_2}$  and  $e^{i\pi\hat{Q}_3}$ , respectively.

*Degeneracy of parafermionic states.* For a given total charge ( $Q_T$ ), the degeneracy of the low-energy Hilbert space of the trijunction is expected to be  $2m$ . Here we propose a setup (depicted in Fig. 3), involving QADs and two external fractional QH edge modes, to directly observe the degenerate subspace. The external fractional modes act as leads from which fractional quasiparticles may tunnel into the trijunction. The Hamiltonian of the two edge modes is given by  $H_a = (mv/4\pi) \int dx [\partial_x \phi_a]^2 - V_a \int dx \partial_x \phi_a$ , where  $V_a$  is the voltage on  $\phi_a$  ( $a = s, d$ ). The quasiparticle tunneling from the edges to the trijunction is described by,

$$H_{\text{qp}} = \sum_{a=s,d} \tilde{\eta}_a e^{i\phi_a} \Gamma_a^\dagger + \text{h.c.} \quad (23)$$

As pointed above, the representation of the PF mode has to be appropriately chosen so that fractional charge only tunnels across the bulk of a QH state, and not across vacuum. If the charging energy for the trijunction is large, then only cotunneling processes are allowed at low energies. These are described by  $H_{\text{ct}} = \eta_c \Gamma_1 \Gamma_0^\dagger e^{-i\phi_d} e^{i\phi_s} + \text{h.c.}$ , where  $\Gamma_0$  is the PF located inside the trijunction and  $\Gamma_1$  is the PF located at a domain wall between a superconductor and tunneling segment (cf. Fig. 3). We assume that quasiparticles may also tunnel between the two modes directly (without involving the trijunction). Such processes are described by  $H_{\text{dir}} = \eta_d e^{-i\phi_d} e^{i\phi_s} + \text{h.c.}$ . Then the total tunneling Hamiltonian is  $H_{\text{dir}} + H_{\text{ct}} = (\eta_d + \eta_c \Gamma_1 \Gamma_0^\dagger) e^{-i\phi_d} e^{i\phi_s} + \text{h.c.}$ , which induces a finite current from the source  $S$  to the drain  $D$  in Fig. 3. The tunneling current may be evaluated in the limit of weak tunneling, following the analysis of Wen [70], as

$$I_t = \frac{|\eta_{\text{eff}}|^2}{v^{2\nu}} \frac{2\pi\nu}{\Gamma(2\nu)} (\nu |V_1 - V_2|)^{2\nu-1}, \quad (24)$$

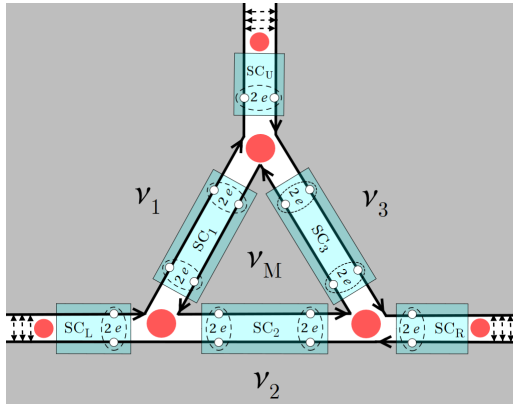


FIG. 4. Multiple trijunctions may be connected to form complex parafermionic networks. The figure depicts a combination of three trijunctions, with a quantum Hall island enclosed only by parafermionic zero modes.

where  $\eta_{\text{eff}}$  is the eigenvalue of  $\eta_d + \eta_c \Gamma_1 \Gamma_0^\dagger$ . As shown earlier, the operator  $\Gamma_j \Gamma_0^\dagger$  depends on  $e^{i\pi \hat{Q}_j}$  ( $e^{i\pi \hat{Q}_1}$  for the setup in Fig. 3). This implies that the current  $I_t$  between the edge modes is sensitive to the state of the trijunction, which may be labelled using  $e^{i\pi \hat{Q}_1}$ . In fact, the state of the trijunction would be projected to an eigenstate of  $e^{i\pi \hat{Q}_1}$  upon measurement of the tunneling current ( $I_t$ ).

The QADs in the setup shown in Fig. 3 may be used to apply the operator  $e^{i\pi \hat{Q}_2}$  to the state of the trijunction, which induces a transition between the degenerate states labelled by  $e^{i\pi Q_1}$ . As discussed above, the tunneling current  $I_t$  is expected to change after the application of  $e^{i\pi \hat{Q}_2}$ , as it depends on the state of the trijunction. Therefore, the degeneracy of the trijunction (for a given charge  $Q_T$ ) may be measured by repeatedly monitoring  $I_t$  and applying  $e^{i\pi \hat{Q}_2}$  through the QADs. The number of steps required before  $I_t$  returns to its initial value is the number of degenerate states in the PF Hilbert space.

*Prospects of parafermionic networks.* The PF zero modes, hosted at the center of star junctions, are identical to those realized in line junction setups [2, 3]. However, a crucial advantage of the our proposal is that such junctions may be used as building blocks for constructing complex parafermionic networks. We first note that the connectivity of a single trijunction, depicted in Fig. 1, is higher than the case of a four PF line junction. Such a configuration could be useful for implementing complex operations (such as, braiding [24]) on the PF modes. Go-

ing on to a small number of star junctions may be combined in a myriad of configurations, each of which may be useful for easily implementing a different set of operations. Figure 4 depicts one such configuration involving 3 trijunctions, which involves an QH island surrounded only by PF zero modes. Repeating the mode expansion analysis for such *loop* geometries, we find that the PF states are sensitive to the fractional charge in the bulk of the enclosed QH puddle, which in turn may be manipulated through additional QADs. Configurations involving several such loops could be useful for quantum information applications. Finally, several such junctions may be employed for constructing large PF networks with different topologies, such as a cycle-free Bethe lattice or a two-dimensional honeycomb structure. The braiding properties of PFs moving on such networks depend sensitively on their connectivity [71–73]. Additionally at low-energies, such networks may be described in terms of emergent phases that support even more exotic non-Abelian excitations [5].

*Conclusions.* We have demonstrated that setups involving multi-legged star junctions of fractional quantum Hall states, may serve as a platform which hosts parafermionic zero modes. Specifically, employing a low-energy mode expansion, we showed that a star with odd (even) number of legs supports (does not support) a parafermionic mode at its center. We also proposed setups involving additional quantum anti-dots and fractional edge modes, which facilitate the detection and manipulation of the parafermionic states. The star shaped junction proposed here, could be used as building blocks for constructing complex parafermionic networks, including two-dimensional lattices, which may be quite difficult to realize using just line junctions. A detailed investigation of the emergent physics of such networks is left for the future.

*Acknowledgments.* We acknowledge useful discussions with Kyrylo Snizhko. U. K. was supported by the Raymond and Beverly Sackler Faculty of Exact Sciences at Tel Aviv University and by the Raymond and Beverly Sackler Center for Computational Molecular and Material Science. M.G. was supported by the US-Israel Bi-national Science Foundation (Grant No. 2016224). Y.G. was supported by CRC 183 (project C01), the Minerva Foundation, DFG Grant No. RO 2247/11-1, MI 658/10-1, the German Israeli Foundation (Grant No. I-118-303.1-2018), the Helmholtz International Fellow Award, and by the Italia-Israel QUANTRA grant.

---

[1] J. Alicea and P. Fendley, Topological phases with parafermions: Theory and blueprints, *Annu. Rev. Condens. Matter Phys.* **7**, 119 (2016).

[2] D. J. Clarke, J. Alicea, and K. Shtengel, *Nat. Commun.* **4**, 1348 (2013).

[3] N. H. Lindner, E. Berg, G. Refael, and A. Stern, Fractionalizing Majorana fermions: Non-Abelian statistics on the edges of Abelian quantum Hall states, *Phys. Rev. X* **2**, 041002 (2012).

[4] L. H. Santos and T. L. Hughes, Parafermionic wires at the interface of chiral topological states, *Phys. Rev. Lett.* **118**, 136801 (2017).

[5] R. S. K. Mong, D. J. Clarke, J. Alicea, N. H. Lindner, P. Fendley, C. Nayak, Y. Oreg, A. Stern, E. Berg, K. Shtengel, and M. P. A. Fisher, Universal topological quantum computation from a superconductor-Abelian quantum Hall heterostructure, *Phys. Rev. X* **4**, 011036 (2014).

[6] J. Alicea and A. Stern, Designer non-Abelian anyon platforms: from Majorana to Fibonacci, *Phys. Scr.* **2015**, 014006 (2015).

[7] D. J. Clarke, J. Alicea, and K. Shtengel, *Nat. Phys.* **10**, 877 (2013).

[8] M. Cheng, Superconducting proximity effect on the edge of fractional topological insulators, *Phys. Rev. B* **86**, 195126 (2012).

[9] M. Burrello, B. van Heck, and E. Cobanera, Topological phases in two-dimensional arrays of parafermionic zero modes, *Phys. Rev. B* **87**, 195422 (2013).

[10] A. Vaezi, Fractional topological superconductor with fractionalized Majorana fermions, *Phys. Rev. B* **87**, 035132 (2013).

[11] F. Zhang and C. L. Kane, Time-reversal-invariant  $\mathbb{Z}_4$  fractional Josephson effect, *Phys. Rev. Lett.* **113**, 036401 (2014).

[12] M. Cheng and R. Lutchyn, Fractional Josephson effect in number-conserving systems, *Phys. Rev. B* **92**, 134516 (2015).

[13] Y. Kim, D. J. Clarke, and R. M. Lutchyn, Coulomb blockade in fractional topological superconductors, *Phys. Rev. B* **96**, 041123 (2017).

[14] B. Beri and N. R. Cooper, Topological Kondo effect with Majorana fermions, *Phys. Rev. Lett.* **109**, 156803 (2012).

[15] A. Altland and R. Egger, Multiterminal Coulomb-Majorana junction, *Phys. Rev. Lett.* **110**, 196401 (2013).

[16] B. Beri, Majorana-Klein hybridization in topological superconductor junctions, *Phys. Rev. Lett.* **110**, 216803 (2013).

[17] K. Snizhko, F. Buccheri, R. Egger, and Y. Gefen, Parafermionic generalization of the topological Kondo effect, *Phys. Rev. B* **97**, 235139 (2018).

[18] M. Gau, S. Plugge, and R. Egger, Quantum transport in coupled Majorana box systems, *Phys. Rev. B* **97**, 184506 (2018).

[19] Y. Herasymenko, K. Snizhko, and Y. Gefen, Universal quantum noise in adiabatic pumping, *Phys. Rev. Lett.* **120**, 226802 (2018).

[20] C. J. Pedder, T. Meng, R. P. Tiwari, and T. L. Schmidt, Missing shapiro steps and the  $8\pi$ -periodic Josephson effect in interacting helical electron systems, *Phys. Rev. B* **96**, 165429 (2017).

[21] A. E. Svetogorov, D. Loss, and J. Klinovaja, Insulating regime of an underdamped current-biased Josephson junction supporting  $\mathbb{Z}_3$  and  $\mathbb{Z}_4$  parafermions, *Phys. Rev. B* **103**, L180505 (2021).

[22] C. Nayak, S. H. Simon, A. Stern, M. Freedman, and S. Das Sarma, Non-Abelian anyons and topological quantum computation, *Rev. Mod. Phys.* **80**, 1083 (2008).

[23] P. Bonderson, M. Freedman, and C. Nayak, Measurement-only topological quantum computation, *Phys. Rev. Lett.* **101**, 010501 (2008).

[24] H. Zheng, A. D. Dua, and L. Jiang, Measurement-only topological quantum computation without forced measurements, *New J. Phys.* **18**, 123087 (2016).

[25] A. Hutter and D. Loss, Quantum computing with parafermions, *Phys. Rev. B* **93**, 125105 (2016).

[26] A. Dua, B. Malomed, M. Cheng, and L. Jiang, Universal quantum computing with parafermions assisted by a half-fluxon, *Phys. Rev. B* **100**, 144508 (2019).

[27] A. Carmi, Y. Herasymenko, E. Cohen, and K. Snizhko, Bounds on nonlocal correlations in the presence of signaling and their application to topological zero modes, *New J. Phys.* **21**, 073032 (2019).

[28] S. Groenendijk, A. Calzona, H. Tschirhart, E. G. Idrisov, and T. L. Schmidt, Parafermion braiding in fractional quantum Hall edge states with a finite chemical potential, *Phys. Rev. B* **100**, 205424 (2019).

[29] L. A. Landau, S. Plugge, E. Sela, A. Altland, S. M. Albrecht, and R. Egger, Towards realistic implementations of a Majorana surface code, *Phys. Rev. Lett.* **116**, 050501 (2016).

[30] C. Knapp, J. I. Väyrynen, and R. M. Lutchyn, Number-conserving analysis of measurement-based braiding with Majorana zero modes, *Phys. Rev. B* **101**, 125108 (2020).

[31] L. Fidkowski and A. Kitaev, Effects of interactions on the topological classification of free fermion systems, *Phys. Rev. B* **81**, 134509 (2010).

[32] A. M. Turner, F. Pollmann, and E. Berg, Topological phases of one-dimensional fermions: An entanglement point of view, *Phys. Rev. B* **83**, 075102 (2011).

[33] X. Chen, Z.-C. Gu, and X.-G. Wen, Complete classification of one-dimensional gapped quantum phases in interacting spin systems, *Phys. Rev. B* **84**, 235128 (2011).

[34] N. Schuch, D. Pérez-García, and I. Cirac, Classifying quantum phases using matrix product states and projected entangled pair states, *Phys. Rev. B* **84**, 165139 (2011).

[35] L. H. Santos, Parafermions in hierarchical fractional quantum Hall states, *Phys. Rev. Research* **2**, 013232 (2020).

[36] M. Barkeshli and X.-L. Qi, Synthetic topological qubits in conventional bilayer quantum Hall systems, *Phys. Rev. X* **4**, 041035 (2014).

[37] M. Barkeshli, C.-M. Jian, and X.-L. Qi, Twist defects and projective non-Abelian braiding statistics, *Phys. Rev. B* **87**, 045130 (2013).

[38] M. Barkeshli, Y. Oreg, and X.-L. Qi, Experimental proposal to detect topological ground state degeneracy, *arXiv:1401:3750* (2014).

[39] J. Klinovaja, A. Yacoby, and D. Loss, Kramers pairs of Majorana fermions and parafermions in fractional topological insulators, *Phys. Rev. B* **90**, 155447 (2014).

[40] C. P. Orth, R. P. Tiwari, T. Meng, and T. L. Schmidt, Non-Abelian parafermions in time-reversal-invariant interacting helical systems, *Phys. Rev. B* **91**, 081406 (2015).

[41] J. Klinovaja and D. Loss, Fractional charge and spin states in topological insulator constrictions, *Phys. Rev. B* **92**, 121410 (2015).

[42] Y. Peng, Y. Vinkler-Aviv, P. W. Brouwer, L. I. Glazman, and F. von Oppen, Parity anomaly and spin transmutation in quantum spin hall Josephson junctions, *Phys. Rev. Lett.* **117**, 267001 (2016).

[43] K. Laubscher, D. Loss, and J. Klinovaja, Fractional topological superconductivity and parafermion corner states, *Phys. Rev. Research* **1**, 032017 (2019).

[44] C. Fleckenstein, N. T. Ziani, and B. Trauzettel,  $\mathbb{Z}_4$  parafermions in weakly interacting superconducting constrictions at the helical edge of quantum spin Hall insulators, *Phys. Rev. Lett.* **122**, 066801 (2019).

[45] P. Fendley, Parafermionic edge zero modes in  $\mathbb{Z}_n$ -

invariant spin chains, *Journal of Statistical Mechanics: Theory and Experiment* **2012**, 11020 (2012).

[46] Y. Oreg, E. Sela, and A. Stern, Fractional helical liquids in quantum wires, *Phys. Rev. B* **89**, 115402 (2014).

[47] J. Klinovaja and D. Loss, Parafermions in an interacting nanowire bundle, *Phys. Rev. Lett.* **112**, 246403 (2014).

[48] J. Klinovaja and D. Loss, Time-reversal invariant parafermions in interacting Rashba nanowires, *Phys. Rev. B* **90**, 045118 (2014).

[49] M. Thakurathi, D. Loss, and J. Klinovaja, Floquet majorana fermions and parafermions in driven Rashba nanowires, *Phys. Rev. B* **95**, 155407 (2017).

[50] A. Chew, D. F. Mross, and J. Alicea, Fermionized parafermions and symmetry-enriched Majorana modes, *Phys. Rev. B* **98**, 085143 (2018).

[51] L. Mazza, F. Iemini, M. Dalmonte, and C. Mora, Non-topological parafermions in a one-dimensional fermionic model with even multiplet pairing, *Phys. Rev. B* **98**, 201109 (2018).

[52] F. Ronetti, D. Loss, and J. Klinovaja, Clock model and parafermions in Rashba nanowires, *Phys. Rev. B* **103**, 235410 (2021).

[53] K. Snizhko, R. Egger, and Y. Gefen, Measurement and control of a Coulomb-blockaded parafermion box, *Phys. Rev. B* **97**, 081405 (2018).

[54] Y. Herasymenko, K. Snizhko, and Y. Gefen, Universal quantum noise in adiabatic pumping, *Phys. Rev. Lett.* **120**, 226802 (2018).

[55] S. Trebst, M. Troyer, Z. Wang, and A. W. W. Ludwig, A short introduction to Fibonacci anyon models, *Progress of Theoretical Physics Supplement* **176**, 384 (2008).

[56] E. M. Stoudenmire, D. J. Clarke, R. S. K. Mong, and J. Alicea, Assembling Fibonacci anyons from a  $\mathbb{Z}_3$  parafermion lattice model, *Phys. Rev. B* **91**, 235112 (2015).

[57] J. Alicea, Y. Oreg, G. Refael, F. von Oppen, and M. P. A. Fisher, Non-Abelian statistics and topological quantum information processing in 1d wire networks, *Nature Physics* **7**, 412 (2011).

[58] B. van Heck, A. R. Akhmerov, F. Hassler, M. Burrelo, and C. W. J. Beenakker, Coulomb-assisted braiding of Majorana fermions in a Josephson junction array, *New J. Phys.* **14**, 035019 (2012).

[59] J. Li, T. Neupert, B. A. Bernevig, and A. Yazdani, Manipulating Majorana zero modes on atomic rings with an external magnetic field, *Nat. Commun.* **7**, 10395 (2016).

[60] M. Trif and P. Simon, Braiding of Majorana fermions in a cavity, *Phys. Rev. Lett.* **122**, 236803 (2019).

[61] M. Alvarado, A. Iks, A. Zazunov, R. Egger, and A. L. Yeyati, Boundary Green's function approach for spinful single-channel and multichannel Majorana nanowires, *Phys. Rev. B* **101**, 094511 (2020).

[62] O. Deb, K. Sengupta, and D. Sen, Josephson junctions of multiple superconducting wires, *Phys. Rev. B* **97**, 174518 (2018).

[63] L. Peralta Gavensky, G. Usaj, and C. A. Balseiro, Topological phase diagram of a three-terminal Josephson junction: From the conventional to the Majorana regime, *Phys. Rev. B* **100**, 014514 (2019).

[64] J. S. Meyer and M. Houzet, Conductance quantization in topological Josephson trijunctions, *Phys. Rev. B* **103**, 174504 (2021).

[65] T. Jonckheere, J. Rech, A. Zazunov, R. Egger, A. L. Yeyati, and T. Martin, Giant shot noise from Majorana zero modes in topological trijunctions, *Phys. Rev. Lett.* **122**, 097003 (2019).

[66] X. G. Wen, Electrodynamical properties of gapless edge excitations in the fractional quantum Hall states, *Phys. Rev. Lett.* **64**, 2206 (1990).

[67] Our results are also valid (qualitatively) for a trijunction comprising the boundary of spin-unpolarized  $\nu = \frac{2}{3}$  QH puddles. In this case, *s*-wave superconducting segments may be employed to gap out the counter-propagating edge modes.

[68] See Supplemental Material for further details.

[69] C. Chen and F. J. Burnell, Tunable splitting of the ground-state degeneracy in quasi-one-dimensional parafermion systems, *Phys. Rev. Lett.* **116**, 106405 (2016).

[70] X.-G. Wen, Edge transport properties of the fractional quantum Hall states and weak-impurity scattering of a one-dimensional charge-density wave, *Phys. Rev. B* **44**, 5708 (1991).

[71] T. Maciazek and A. Sawicki, Non-Abelian quantum statistics on graphs, *Commun. Math. Phys.* **371**, 921 (2019).

[72] T. Maciazek and B. H. An, Universal properties of anyon braiding on one-dimensional wire networks, *Phys. Rev. B* **102**, 201407 (2020).

[73] B. H. An and T. Maciazek, Geometric presentations of braid groups for particles on a graph, *Comm. Math. Phys.* **384**, 1109 (2021).

# Supplementary Material for “Parafermions in a multi-legged geometry: Towards a scalable parafermionic network”

Udit Khanna,<sup>1,2,3</sup> Moshe Goldstein,<sup>1</sup> and Yuval Gefen<sup>2</sup>

<sup>1</sup>Raymond and Beverly Sackler School of Physics and Astronomy, Tel Aviv University, Tel Aviv 6997801, Israel

<sup>2</sup>Department of Condensed Matter Physics, Weizmann Institute of Science, Rehovot 76100, Israel

<sup>3</sup>Present Affiliation: Department of Physics, Bar-Ilan University, Ramat Gan 52900, Israel

This supplemental material provides additional details regarding our analysis of the trijunction.

## Parafermions in the Trijunction

As described in the main text, the  $j^{\text{th}}$  superconducting segment ( $j = 1, 2, 3$ ) imposes the following boundary condition on the chiral modes entering ( $\phi_{j-1}$ ) and emanating ( $\phi_j$ ) from it,

$$\phi_j(x=0, t) + \phi_{j-1}(x=L_{j-1}, t) = \frac{2\pi}{m} \hat{N}_j, \quad (\text{S1})$$

where  $j = 0$  has been identified with  $j = 3$  for brevity. Additionally, we use the convention that  $x$  increases along the direction of propagation for each chiral mode. Note that physically, the boundary condition (S1) implies that the current entering the superconductor is equal in magnitude and opposite in sign to the current exiting the superconductor. To find the spectrum of the problem, we consider the standard mode expansion for right-moving chiral fields for the three chirals,

$$\begin{aligned} \phi_j(x, t) = & \varphi_j + A_j p_{\varphi_j} (vt - x) + \\ & \sum_{n>0} \left[ B_{nj} a_{nj} e^{-iq_{nj}(vt-x)} + \text{h.c.} \right]. \end{aligned} \quad (\text{S2})$$

Here,  $A_j$  and  $B_{nj}$  are  $c$ -numbers,  $\varphi_j$ ,  $p_{\varphi_j}$  are the conjugate pair of zero-mode operators, and  $a_{nj}$  is the annihilation operator for the  $n^{\text{th}}$  ( $n \geq 1$ ) bosonic excitation with wavevector  $q_{nj}$ . Using (S1) in (S2), we find,

$$\begin{aligned} & \varphi_j + A_j p_{\varphi_j} vt = \\ & -\varphi_{j-1} - A_{j-1} p_{\varphi_{j-1}} (vt - L_{j-1}) + \frac{2\pi}{m} \hat{N}_j, \quad (\text{S3}) \\ & \sum_n B_{nj} a_{nj} e^{-iq_{nj}vt} = \\ & - \sum_n B_{nj-1} a_{nj-1} e^{-iq_{nj-1}(vt-L_{j-1})}. \end{aligned} \quad (\text{S4})$$

In order to satisfy (S3) for all time ( $t$ ), we must have  $A_j = 0$ , and  $\varphi_j = \varphi_{j-1} + \frac{2\pi}{m} \hat{N}_j$  for all  $j$ . Solving the latter set of linear equations,

$$\varphi_j = \frac{\pi}{m} (\hat{N}_j + \hat{N}_{j+1} - \hat{N}_{j-1}). \quad (\text{S5})$$

As stated in the main text, here we assume that the edge modes are segments of a single boundary [hence we impose Eq. (3) of the main text]. Therefore, we use a single wavevector  $q_n$  and a single mode operator  $a_n$  for

all three chirals. In this case, (S4) is satisfied for all  $t$  only if

$$B_{nj} a_n = -B_{nj-1} e^{iq_n L_{j-1}} a_n, \quad (\text{S6})$$

which in turn implies

$$\begin{aligned} B_{n3} a_n &= -B_{n2} e^{iq_n L_2} a_n \\ &= B_{n1} e^{iq_n (L_2 + L_1)} a_n \\ &= -B_{n3} e^{iq_n \ell} a_n, \end{aligned} \quad (\text{S7})$$

where  $\ell = \sum_j L_j$  is the total length of the three chirals. Eq. (S7) naturally leads to the quantization condition for the wavevectors,  $q_n = (2n-1) \frac{\pi}{\ell}$ . Using the mode expansion in Eq. (2) of the main text (along with the standard bosonic commutations for  $a_n$ ), we find that

$$B_{nj}^2 = \frac{2\pi}{m\ell} \frac{1}{q_n}. \quad (\text{S8})$$

Collecting everything together, we deduce that the chiral modes must satisfy,

$$\phi_1(x, t) = \varphi_1 + \sqrt{\frac{2}{m}} \sum_{n>0} \left[ \frac{a_n}{\sqrt{2n-1}} e^{-iq_n(vt-x)} + \text{h.c.} \right], \quad (\text{S9})$$

$$\phi_2(x, t) = -\phi_1(x + L_1, t) + \varphi_1 + \varphi_2, \quad (\text{S10})$$

$$\phi_3(x, t) = -\phi_2(x + L_2, t) + \varphi_2 + \varphi_3. \quad (\text{S11})$$

Similarly, using (3) of the main text, we obtain the commutation relations between the zero mode operators,

$$[\varphi_2, \varphi_1] = [\varphi_3, \varphi_2] = \frac{2\pi i}{m} \quad \text{and} \quad [\varphi_1, \varphi_3] = 0. \quad (\text{S12})$$

Using (S5) in (S12), we find that the only non-zero commutation relation between the  $\hat{N}$  operators is

$$[\hat{N}_3, \hat{N}_2] = \frac{im}{\pi}. \quad (\text{S13})$$

Next, we use the mode expansion derived above in the Hamiltonian of the trijunction,  $H = H_{\text{edge}} + H_s + H_t$  [the three components are defined in Eqs. (1), (4) and (5) of the main text]. Since  $H_{\text{edge}}$  depends only on  $\partial_x \phi_j$ , we do not expect the zero mode operators ( $\varphi_j$ ) to affect  $H$ . Indeed, using (S9–S11) we find,

$$H = \sum_{n>0} vq_n (a_n^\dagger a_n + \frac{1}{2}). \quad (\text{S14})$$

In order to show the existence of a localized zero-energy excitation, we need to construct a physical operator (say,  $\tilde{\Gamma}_0$ ) which commutes with  $H$ . Here, “physical” means that  $\tilde{\Gamma}_0$  is only composed of operators corresponding to the local excitations of the effective theory. The low-energy dynamics of the junction is controlled by the bosonic excitations (described by  $a_n$  and  $a_n^\dagger$ ) and the anyonic quasi-hole/quasiparticle excitations (described by  $e^{\mp i\phi_j(x)}$ ). Since the bosonic excitations have finite energy, any zero-energy excitation may only be composed of the vertex operators corresponding to quasi-hole/quasiparticle excitations. We begin the task of writing an explicit form of  $\tilde{\Gamma}_0$  by noting that

$$\begin{aligned} [H, \phi_j(x)] &= \sum_{n_1, n_2 > 0} v q_{n_2} \sqrt{\frac{2}{m}} \frac{1}{\sqrt{2n_1 - 1}} \times \\ &\quad [a_{n_2}^\dagger a_{n_2}, a_{n_1} e^{-iq_{n_1}(vt-x)} + \text{h.c.}] \\ &= -v \sum_{n > 0} \sqrt{\frac{2}{m}} \frac{q_n}{\sqrt{2n - 1}} \left[ a_n e^{-iq_n(vt-x)} - \text{h.c.} \right] \\ &= iv \partial_x \phi_j(x). \end{aligned} \quad (\text{S15})$$

Using (S15) recursively, we find

$$\begin{aligned} [H, (\phi_j(x))^n] &= [H, (\phi_j(x))^{n-1}] \phi_j(x) \\ &\quad + (\phi_j(x))^{n-1} [H, \phi_j(x)] \\ &= iv \partial_x (\phi_j(x))^n. \end{aligned} \quad (\text{S16})$$

(S16) may then be used to show that

$$[H, e^{\phi_j(x)}] = iv \partial_x (e^{\phi_j(x)}). \quad (\text{S17})$$

Noting that the right hand side of (S17) is a total derivative, we have,

$$\left[ H, \int_0^{L_j} dx e^{\phi_j(x)} \right] = iv \left( e^{i\phi_j(L_j)} - e^{i\phi_j(0)} \right). \quad (\text{S18})$$

Since  $H$  commutes with  $\varphi_j$ , we rewrite (S18) as,

$$\begin{aligned} \left[ H, \int_0^{L_j} dx e^{-i\varphi_j} e^{\phi_j(x)} \right] &= iv \left( e^{-i\varphi_j} e^{i\phi_j(L_j)} - e^{-i\varphi_j} e^{i\phi_j(0)} \right) \\ &= iv \left( e^{i(\phi_j(L_j) - \varphi_j)} - e^{i(\phi_j(0) - \varphi_j)} \right). \end{aligned} \quad (\text{S19})$$

In the second equality above, we used the fact that  $[\varphi_j, \phi_j(x)] = 0$ . Employing (S1) and (S9–S11), it is trivial to show that,

$$\phi_j(0, t) - \varphi_j = -[\phi_{j-1}(L_{j-1}, t) - \varphi_{j-1}]. \quad (\text{S20})$$

Finally, using (S19) together with (S20), we find

$$\left[ H, \sum_{j=1}^3 \int_0^{L_j} dx (e^{-i\varphi_j} e^{\phi_j(x)} + \text{h.c.}) \right] = 0. \quad (\text{S21})$$

We emphasize that Eq. (S21) is only valid in the case of an odd number of superconducting segments. In the case of an even-legged junction,  $A_j \neq 0$ , and the Hamiltonian would not be independent of  $\hat{N}_j$ . An equation of the form (S21) would not be valid in such a situation.

Even though the operator in (S21) commutes with  $H$ , we have not reached our goal yet, since  $e^{\mp i\varphi_j}$  (which is a crucial part of this operator) does not describe any physical excitation of the Hilbert space. In order to render it physical, we note that (S20) may be written as

$$\varphi_j + \varphi_{j-1} = \phi_j(0, t) + \phi_{j-1}(L_{j-1}, t). \quad (\text{S22})$$

(S22) motivates us to consider a family of operators of the form

$$\tilde{\Gamma}_{0,k} = e^{i\varphi_k} \sum_{j=1}^3 \int_0^{L_j} dx (e^{-i\varphi_j} e^{\phi_j(x)} + \text{h.c.}), \quad (\text{S23})$$

where  $k = 1, 2, 3$ . Clearly, they satisfy  $[H, \tilde{\Gamma}_{0,k}] = 0$ . Additionally, up to trivial phase factors, the zero-mode operators enter  $\tilde{\Gamma}_{0,k}$  in one of three forms:  $e^{i(\varphi_j + \varphi_k)}$ ,  $e^{2i\varphi_k}$ , or  $e^{i(\varphi_k - \varphi_j)}$ . According to (S22),  $e^{i(\varphi_j + \varphi_k)}$  represents a local pair of quasi-hole and quasiparticle excitations at the boundary of one of the superconducting segments. The second and third forms may also be interpreted in a similar way, since (up to trivial phase factors)  $e^{2i\varphi_k} = e^{i(\varphi_k + \varphi_{k+1})} e^{i(\varphi_k + \varphi_{k-1})} e^{-i(\varphi_{k+1} + \varphi_{k-1})}$ , and  $e^{i(\varphi_k - \varphi_j)} = e^{i(\varphi_k + \varphi_{k+1})} e^{-i(\varphi_j + \varphi_{k+1})}$ . Hence, we conclude that  $\tilde{\Gamma}_{0,k}$  indeed represent physical zero-energy excitations of the system. Note, however, that  $\tilde{\Gamma}_{0,k}$  for different  $k$  are not independent of each other. Indeed, they are related to each other by

$$\tilde{\Gamma}_{0,k_2} = e^{i(\varphi_{k_2} - \varphi_{k_1})} \tilde{\Gamma}_{0,k_1}, \quad (\text{S24})$$

and as we mentioned above,  $e^{i(\varphi_{k_2} - \varphi_{k_1})}$  may be decomposed in terms of physical operators. In other words, the three operators represent the same zero-energy excitation, but with different dressing of quasi-hole-quasiparticle pairs. Therefore, in Eq. (19) of the main text, we define a single zero-energy excitation ( $\tilde{\Gamma}_0$ ), which without loss of generality may be identified with ( $\tilde{\Gamma}_{0,1}$ ).